RESEARCH ARTICLE

VIEW

Single local delivery of 5′-(N-ethylcarboxamido)adenosine depots ameliorates myocardial infarction-induced cardiac dysfunction via the enhancement of mitostasis

Shibo Wei[1] | **Tiep Tien Nguyen**[2] | **Yan Zhang**[1,3] | **Wonyoung Park**[4] |
Nhu-Nam Nguyen[2] | **Jiwoo Kim**[5,6] | **Yunju Jo**[1] | **Chang-Myung Oh**[1] |
Doyoun Kim[5,7] | **Jin Han**[8] | **Ki-Tae Ha**[4] | **Jee-Heon Jeong**[2] | **Dongryeol Ryu**[1] ⬤

[1]Department of Biomedical Science and Engineering, Gwangju Institute of Science and Technology, Gwangju, Republic of Korea

[2]Department of Precision Medicine, Sungkyunkwan University School of Medicine, Suwon, Republic of Korea

[3]Department of Molecular Cell Biology, Sungkyunkwan University School of Medicine, Suwon, Republic of Korea

[4]Department of Korean Medical Science, School of Korean Medicine, Pusan National University, Yangsan, Republic of Korea

[5]Therapeutics & Biotechnology Division, Rare Disease Therapeutics Research Center, Korea Research Institute of Chemical Technology, Daejeon, Republic of Korea

[6]Graduate School of New Drug Discovery and Development, Chungnam National University, Daejeon, Republic of Korea

[7]Department of Pharmacy, Sungkyunkwan University, Suwon, Republic of Korea

[8]Department of Physiology, College of Medicine, Inje University, Busan, Republic of Korea

Correspondence
Dongryeol Ryu, Department of Biomedical Science and Engineering, Gwangju Institute of Science and Technology, Gwangju 61005, Republic of Korea.
Email: dryu@gist.ac.kr

Jee-Heon Jeong, Department of Precision Medicine, Sungkyunkwan University School of Medicine, Suwon 16419, Republic of Korea.
Email: jeeheon@skku.edu

Abstract

Myocardial infarction (MI) stands as a prominent contributor to global mortality. Despite existing therapies, there are notable shortcomings in delivering optimal cardiac support and reversing pathological progression, particularly within early stages. Adenosine presents a promising therapeutic target; however, its clinical utility is impeded by inherent limitations. In this study, an advanced strategy using adenosine agonist is pioneered to ameliorate MI-induced myocardial damage. Herein, an adenosine derivative 5′-(N-ethylcarboxamido) adenosine (NECA) is employed, and its therapeutic efficacy is evaluated via single local delivery into infarcted myocardium following MI. NECA displays remarkable benefits in endothelial cells and cardiomyocytes under both normoxic and hypoxic conditions. Likewise, single localized NECA delivery via newly developed NECA-loaded micro-depots demonstrates advanced improvement in cardiac function and prevention of myocardial damage in a MI mouse model, with notable promotion of angiogenesis and suppression in inflammation, oxi-

---

Shibo Wei and Tiep Tien Nguyen contributed equally to this study.

dation, and apoptosis. Mechanistically, NECA exerts myocardial benefits via the enhancement of mitostasis by triggering AMP-activated protein kinase α (AMPKα) phosphorylation and Peroxisome proliferator-activated receptor gamma coactivator 1-alpha(PGC-1α) activation. These findings highlight the clinical significance of adenosine agonist NECA in cardiac support and recovery, with the single-delivered depots providing an advanced intervention for individuals with critically severe MI in the early phase.

KEYWORDS
adenosine derivative depot, intramyocardial injection, mitostasis, myocardial infarction

1 | INTRODUCTION

Myocardial infarction (MI) remains a global health concern of paramount significance.[1] The cardiac pathological alterations following MI are marked by a complex interplay of diverse processes, including cardiomyocyte death, inflammatory response, and oxidative stress, with persistent or excessive activation resulting in adverse cardiac remodeling and eventual heart failure.[2,3] Currently, clinical interventions on MI mainly aim at symptoms alleviation, rapid revascularization, and complications prevention.[4] However, these strategies tend to focus more on symptom management and the prevention of further cardiac incidents, rather than directly targeting the fundamental pathological alterations.[5] Moreover, considering the compromised state of the heart following MI, particularly in the perioperative period, its heightened sensitivity and vulnerability render it less resilient to stressors, so as medications and surgeries.[6] In this context, interventions aimed at ameliorating the pathological processes during MI progression take on renewed importance. Efficient cardiac support strategies are prone to substantially attenuate MI-induced cardiac injury and enhance cardiac tolerance, holding promising potential to facilitate improved clinical outcomes.[2]

Adenosine is a ubiquitous metabolite recognized for its modulation of intricate cellular functions through distinct subtypes of G protein-coupled receptors.[7] This multifaceted molecule is well documented for its pivotal role in distinct cellular processes, including energy transduction, vasodilation, and immune regulation.[8] Exogenously administered adenosine has demonstrated potential benefits in myocardial recovery, such as microvascular perfusion preservation, oxidative stress mitigation, and calcium homeostasis restoration.[9] However, its clinical application in MI therapy is constrained by certain inherent limitations including short half-life, non-specific actions, and the

potential of side effects affecting other organ systems.[10] To address these challenges, researchers have endeavored to develop distinct patterns of adenosine agonist over the decades.[11] Among them, 5′-(N-ethylcarboxamido) adenosine (NECA) has emerged as a notable candidate, displaying remarkable advancements in terms of stability, potent vasodilatory effects, and anti-inflammatory efficacy.[12] Notably, current investigations also emphasized the vasculogenic impacts of NECA on various tissues,[13,14] indicating its potential on the recovery of cardiac function post-MI via improved perfusion of the infarcted area. Collectively, these distinctive pharmacological profiles of NECA exhibit promising prospects as an effective intervention in the context of MI therapy. However, there is an absence of investigations indicating its curative effects and underlying mechanisms.

Intramyocardial injection (IMI), a well-established technique, finds wide-ranging application in cardiovascular research. IMI has been employed, for instance, in heart failure alleviation via stem cell injection,[15] and cardiac function enhancement via the delivery of drugs or growth factors using diverse carriers, including synthetic hydrogels, microparticles, and nanoparticles.[16] Whereas IMI is not without its associated risks such as bleeding and myocardial injury, contemporary research underscores multiple advantages of IMI, encompassing its rapid onset, direct action, and targeted therapy, demonstrating conspicuous utility and clinical relevance in the treatment of patients. Notably, IMI of mRNA, stem cells, and drugs has recently shown promising curative efficacies in clinical trials involving patients with congenital heart defects, ischemic heart disease, and cardiomyopathies, highlighting its potential in cardiac support and treatment in MI. Conversely, it is noteworthy that certain clinical trials have also failed to demonstrate a clear improvement in cardiac recovery among patients with advanced heart failure.[17] As such, the development of more effective drugs for

IMI to preserve cardiac function and impede pathological progression in the early phase of MI holds significant necessities.

In our study, we employed an adenosine agonist NECA and validated its potential benefits in myocardial cells. We fabricated NECA-loaded poly(lactic-co-glycolic acid) (PLGA) micro-depots and substantiated its curative efficacy in ameliorating cardiac dysfunction and myocardial damage during the early phase of MI. The sustained release of NECA from single intramyocardially delivered depots exhibited multifaced benefits in mitigating diverse pathological progressions and enhancing angiogenesis. Mechanistic investigations revealed its capacity to augment mitostasis through AMP-activated protein kinase α (AMPKα) phosphorylation and PGC-1α activation. Collectively, our findings emphasize the clinical significance of NECA and offer novel insights for advancing MI treatment.

2 | EXPERIMENTAL/METHODS

2.1 | Fabrication and characterization of NECA depots

NECA-loaded PLGA (LA:GA 50:50, 38–54 kDa) micro-depots (NEDepot) were fabricated using oil-in-oil emulsion method. Briefly, 0.5 mg of NECA and 400 mg of PLGA were dissolved in 0.4 mL of methanol and 1.6 mL of acetonitrile, respectively, which was vigorously mixed to form solution A (internal oil phase). The external oil phase (solution B) was prepared by mixing liquid paraffin (112 mL), petroleum ether (80 mL) and Span 80 (8 mL). Next, 2 mL solution A was emulsified in 20 mL solution B at 25,000 rpm for 5 min at room temperature (RT). The resulting emulsion was stabilized in 180 mL solution B while stirring at 600 rpm and 35°C for 2 days in a hood to allow complete evaporation of organic solvents, except for liquid paraffin. Thereafter, petroleum ether (100 mL) was added to the resulting solution containing hardened NEDepot, which was transferred into 50 mL tubes for centrifugation at 2000 rpm for 5 min. The depots were thoroughly washed in petroleum ether (40 mL) for more three times and let to be dried at RT for 1–2 days. The depots were further dispersed in distilled water, filtered via 40 μm membrane, and lyophilized to obtain completely dried powder.

The morphology of NEDepot was characterized using a field emission scanning electron microscope after a thin layer coating of platinum. The size of NEDepot was measured using the ImageJ software. The loading capacity and release pattern of NECA were determined using the previously developed High-Performance Liquid Chromatography (HPLC) method.[14] For loading capacity test, 5–10 mg of NEDepot was dissolved in 0.5 mL dichloromethane, and vigorously mixed with 1 mL water containing 0.1% phosphoric acid. NECA was extracted in aqueous layer after centrifugation at 14,000 rpm for 3 min. The release of NECA was performed by incubating 15–50 mg of NEDepot in 0.2 mL of phosphate-buffered saline (PBS) (pH 7.4) in a shaking condition at 100 rpm and 37°C. The NEDepot was pelleted, and supernatant was sampled daily for 18 days. The stability of NEDepot was assessed by storing lyophilized NEDepot powder, labeled with Coumarin-6, at 4°C for 18 months or at RT (20°C–25°C) for 6 months. Particle morphology and aggregation were evaluated using fluorescence microscopy, while NECA levels in NEDepot were quantified using HPLC to determine drug stability over the storage period.

2.2 | Mice experiments

MI mouse model (10-week-old C57BL/6 male mouse) was set up via left coronary artery ligation as previously described.[18] For NEDepot-treated mice, NEDepot (diluted in PBS) was injected within the infarcted myocardium, at three sites with 10 μL each. The three injection sites formed an equilateral triangle, and the spacing was about 1.5 mm. All animal experiments adhered to ethical guidelines and received approval from the Institutional Animal Care and Use Committee (IACUC) of Gwangju Institute of Science and Technology, with the protocol number designated as GISTIACUC-2023-040.

2.3 | Molecular docking simulation of NECA into AMPK

To prepare for the docking simulation, we extracted the gamma subunit of AMPK from the crystal structure of the AMPK complex (PDB ID 4EAI) using PyMol software (version 1.8).[19] AutoDockTools software package was then used to prepare the AMPKγ subunit for docking simulation, which included simulating protonation states and performing energy minimization.[20] The 3D coordinate of NECA were generated using the Open Babel software. We performed the molecular docking simulation using Autodock vina software (version 1.2.0) on the AMP-binding regions of AMPKγ subunit. The search grid was set to $35.4 \times 25.3 \times 25.3$ Å with position of –20, 5, and –12 with an exhaustiveness of 10 and 10 modes. All the structures were visualized using PyMol.

2.4 | CRISPR-mediated genome editing

CRISPR-mediated genome editing was conducted as previously described.[21] Target sequences for AMPKγ2 were designed via CHOPCHOP (http://chopchop.cbu.uib.no). The single guide RNAs (sgRNAs) applied in this study are listed in Table S1. Complementary oligonucleotides with BsmBI restriction sites for sgRNAs were synthesized (Bionics) and cloned into a lentiCRISPR v2 vector (Addgene).

3 | RESULTS

3.1 | NECA preserved the viability and functionality of endothelial cells and cardiomyocytes

In consideration of the revascularized potential of NECA observed in the prior study,[14] we initially verified the angiogenic effects of NECA in endothelial cells (ECs). Human umbilical vein endothelial cells (HUVECs) were subjected to NECA treatment at varying concentrations under starving and $CoCl_2$-mimiked hypoxic conditions, which demonstrated an augmentation of HUVECs proliferation in a dose-dependent manner. Specifically, NECA evidently enhanced HUVECs viability at 24 and 72 h of starvation (Figure 1A), while preventing cell death from hypoxic injury in 24 h (Figure 1B). Additionally, NECA treatment significantly promoted angiogenic properties of HUVECs, visualized by tube-like formation (Figure 1C) and migration assays (Figure 1E). Evident tube structures and increased total tube length were observed in NECA-treated HUVECs at the concentrations of NECA above 10 μM (Figure 1D). NECA exhibited a dose-dependent enhancement in HUVECs migration, reaching approximately a 10-fold increase compared to vehicle-treated group at a concentration of 100 μM (Figure 1F). These findings highlight the protective effects of NECA on HUVECs while improving its angiogenic functionalities.

To investigate the potential benefits of NECA on cardiomyocytes, we assessed H9c2 cell viability treated with NECA under normoxic and $CoCl_2$-mimicked hypoxic conditions. NECA demonstrated no cytotoxicity in H9c2 cells at the concentration below 100 μM (Figure 1G), while ameliorating hypoxic injury, evident in enhanced viability (Figure 1H) and proliferative property (Figure S1). In consist, $CoCl_2$-treated H9c2 cells demonstrated elevated mRNA expression of an apoptotic regulator *Bax* and inflammatory genes *Il1b*, *Il6*, and *Tnf* (Figure 1I), while these increases were evidently inhibited by NECA in a time-dependent manner. These findings indicate that NECA effectively protects cardiomyocytes from hypoxic-induced apoptosis and inflammatory response, both critical for maintaining cardiac function in MI progression.

3.2 | NECA depots were fabricated for local administration via IMI

To enhance the therapeutic efficacy of NECA in the early phase of MI, we optimized the NECA delivery system by developing NEDepot using the degradable biomaterial PLGA for conducting localized NECA administration (Figure 2A). NEDepot was fabricated as spherical with the most size range of 10–40 μm to limit additional injury during IMI (Figure 2B,C). NECA was found to be effectively loaded in NEDepot, as evidenced by high encapsulation efficiency (80.34 ± 2.03%), with an actual loading capacity of 0.100 ± 0.003% determined by HPLC method (Figure 2D). Likewise, NEDepot showed a rapid release of roughly 40% at day 1 and 30% at day 2, followed by a sustained release pattern of less than 10% per day for up to 18 days (Figure 2E). Notably, NEDepot demonstrated excellent lyophilization properties, forming a fine powder that preserved particle morphology, prevented degradation, and maintained drug loading over extended periods. The lyophilized NEDepot retained their structural integrity without aggregation, and NECA levels remained stable (>93% of the initial content) after long-term storage at 4°C or RT (Figure S2A,B), highlighting its superior stability.

In addition, the biosafety of NEDepot was assessed in vitro using H9c2 cells. NEDepot exhibited no cytotoxicity over a 3-day period while promoting cell proliferation to a certain extent (Figure S2C). Consistently, NEDepot demonstrated excellent biosafety, as evidenced by the absence of genotoxic effects (Figure S2D,E) and the lack of oxidative stress induction (Figure S2F), in stark contrast to the positive control, doxorubicin. Furthermore, we demonstrated that NEDepot escaped phagocytosis activity of RAW 264.7 macrophages in non-stimulated and lipopolysaccharide (LPS)-stimulated conditions. Macrophages attached to the NEDepot surface within 3 h of incubation and subsequently formed extensive clusters by 24 h, however, they demonstrated an inability to engulf and eliminate NEDepot (Figure 2F). Furthermore, NEDepot exhibited favorable biocompatibility features. We assessed the expression of inflammation-related genes in macrophages following a 24-h co-incubation. Blank depots provoked the upregulation of inflammatory genes, including *Il1b*, *Il6*, *Il10*, and *Tnf*, in both naïve and LPS-preactivated macrophages. Conversely, NEDepot reversed these adverse impacts, while evidently
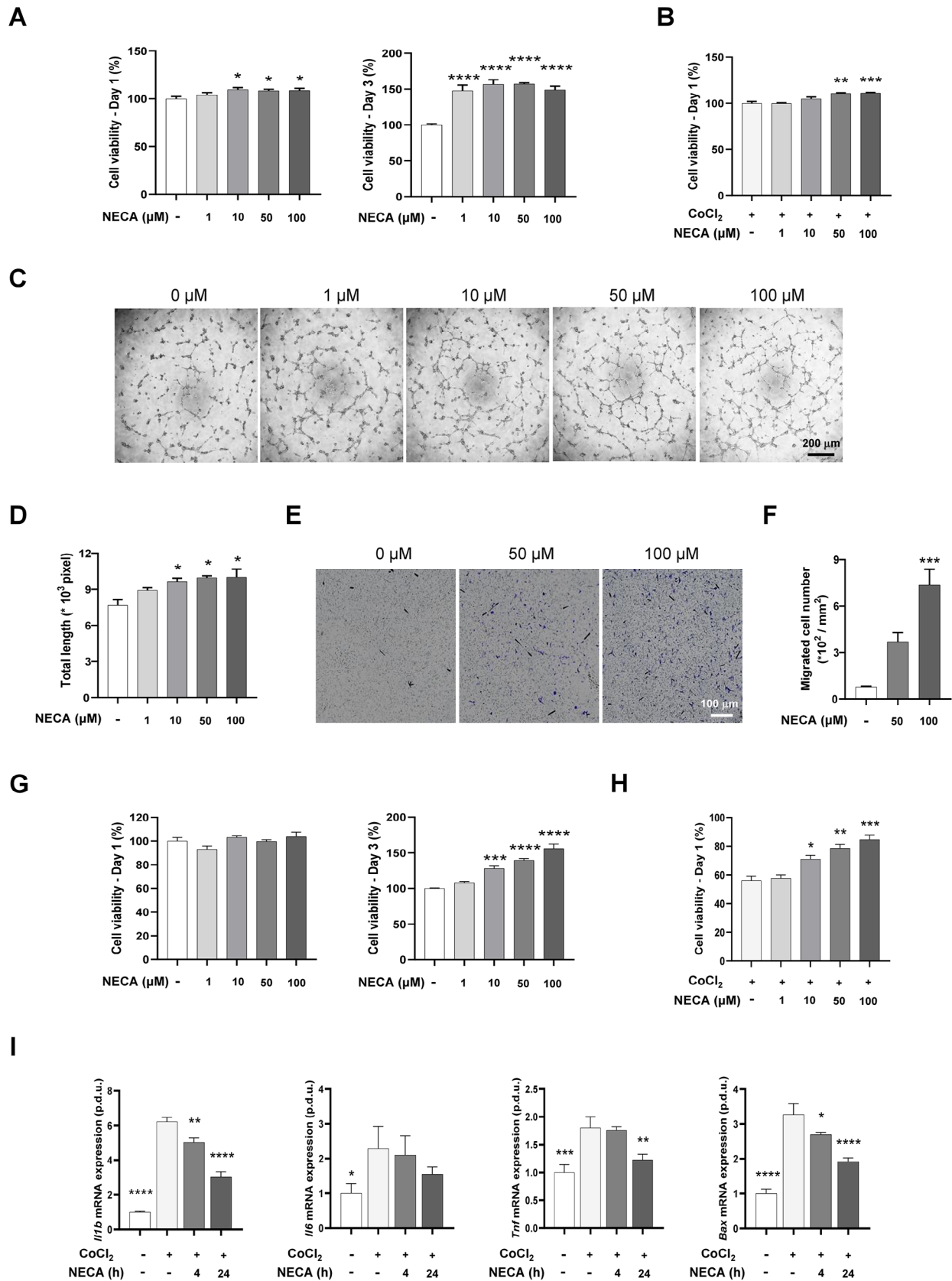
FIGURE 1 5′-(N-ethylcarboxamido) adenosine (NECA) enhanced angiogenetic effects in endothelial cells and protected cardiomyocytes from hypoxic injury. (A) Cell viability assay of human umbilical vein endothelial cells (HUVECs) under normoxic condition treated with NECA for 24 and 72 h ($n = 5$). (B) Cell viability assay of HUVECs under CoCl$_2$-mimiced hypoxic condition treated with NECA for 24 h ($n = 5$). (C and D) Tube-like formation assay of NECA-treated HUVECs under normoxic condition ($n = 3$). Scale bar: 100 μm. (E and F) Cell migration

promoting the expression of anti-inflammatory gene *Tnfaip6* (Figure 2G).

3.3 | Local NEDepot administration prevented cardiac dysfunction in the early phase of MI

In consideration of the potential benefits of NEDepot in MI, we examined its cardioprotective effects in a MI mouse model (Figure 3A). To confirm the success of IMI, we labeled NEDepot with Cy5.5 and visualized by In Vivo Imaging Spectrum System after injection (Figure 3B). To optimize the conditions of NEDepot for cardiac recovery in vivo, we evaluated the systolic function of left ventricular (LV) at 10-day post-MI in mice with different treatments. Echocardiogram showed a significant decline in ejection fraction (EF) and fraction shortening (FS) in MI groups, which were reserved by both free NECA and NEDepot treatment, with notable enhancement observed with NEDepot at 0.45 mg (in 30 μL) (Figure 3C). To confirm the biosafety of NEDepot in vivo, a pre-experiment was conducted to evaluate multiple indices in normal mice treated with vehicle or NEDepot (0.45 mg in 30 μL) at 10 days post-injection. Both groups showed no significant alterations in body weight and food intake (Figure S3A,B). Likewise, NEDepot injection did not impair LV systolic function or induce structural remodeling (Figure S3C,D). NEDepot also displayed a favorable systemic safety profile, as evidenced by its lack of impact on cardiac, hepatic, and renal mass (Figure S3E), alongside unaltered serum cTnI levels (Figure S3F), emphasizing its biocompatibility and non-cytotoxicity across multiple organ systems. Next, we conducted a systematic evaluation of the cardiac index indicative of the cardiac phenotype alterations among Sham, MI, and MI with NEDepot (0.45 mg in 30 μL) treatment group (referred to as MI + NEDepot). Electrocardiography analysis revealed milder alterations in heart rate (HR) in NEDepot-treated MI mice (Figure 3D). Vehicle-treated MI mice exhibited significantly extended and differential cardiac rhythm, while the enhanced incidence of arrhythmia was notably reversed by NEDepot treatment 10-day post-MI (Figure 3E). Additionally, NEDepot-treated MI mice exhibited improved cardiac function close to the level of sham group, while vehicle-treated MI mice severely suffered with a severe reduction in EF and FS (Figures 3F and S4A). The relative LV mass

of MI group decreased compared to that of Sham but was attenuated by NEDepot treatment (Figure 3G). Meanwhile, MI mice exhibited evident myocardial remodeling, particular of interventricular septum (Figures 3H and S4B). However, the remodeling was evidently milder in NEDepot-treated MI mice. Notably, hemodynamics assessment in right ventricle revealed a significant reduction in MI mice, which was attenuated by NEDepot treatment (Figure 3I). These data substantiate the effective cardioprotective effects of NEDepot against MI-induced cardiac dysfunction in the early phase.

3.4 | NEDepot administration altered gene related to cardiac adaptability, mitochondrial metabolism, inflammation, and oxidative stress

To get further insight into the mechanisms underlying the observed cardioprotective effects of NEDepot, we performed transcriptome profiling using gene set enrichment analysis (GSEA), an unbiased method (Figure 4A). To determine the effect of NEDepot, we adopted a strategy of comparing both the MI + NEDepot group and the healthy Sham group to the MI group in the disease state. In overall, similar to the phenotype observed in mice with improved symptoms, we found that the transcriptomic trends of NEDepot were similar to those of the normal sham group. Both gene sets related to cardiac function and homeostasis (shaded in orange) and those related to antioxidants (shaded in light blue) had positive normalized enrichment scores (NES) in the NEDepot group, as well as in the normal Sham group. However, all gene sets related to inflammation (shaded in purple) were enriched with negative NES in the MI group (Figure 4A,B). It is interesting to note that the gene sets related to mitochondrial function, which were not significantly observed in the Sham group, were enriched in the MI + NEDepot group, implying that NEDepot has a mode-of-action that regulates mitochondrial gene expression. To comprehend the connections among altered genes indicated by GSEA analysis, we constructed two gene networks based on their correlation, which was generated by using the gene expression values in the normal Sham condition as the baseline for both groups, and the changes in gene expression values were applied to the MI condition and the treatment condition using NEDepot. Interestingly, the

---

assay of NECA-treated HUVECs stained with crystal violet ($n = 4$). Scale bar: 100 μm. (G and H) Cell viability assay of NECA-treated cardiomyocytes under normoxic (A) and hypoxic (B) conditions ($n = 4$). (I) The mRNA expression level of inflammation and cell death markers in cardiomyocytes under hypoxic condition in response to NECA treatment ($n = 3$). *Il1b*: interleukin 1 beta, *Il6*: interleukin 6, *Tnf*: tumor necrosis factor, *Bax*: BCL2-associated X. $*p < .05$, $**p < .01$, $***p < .001$, $****p < .0001$ versus untreated control (A–G) or $CoCl_2$-treated group (H and I). Data represent the mean ± Standard Error of the Mean (SEM), by one-way analysis of variance (ANOVA).
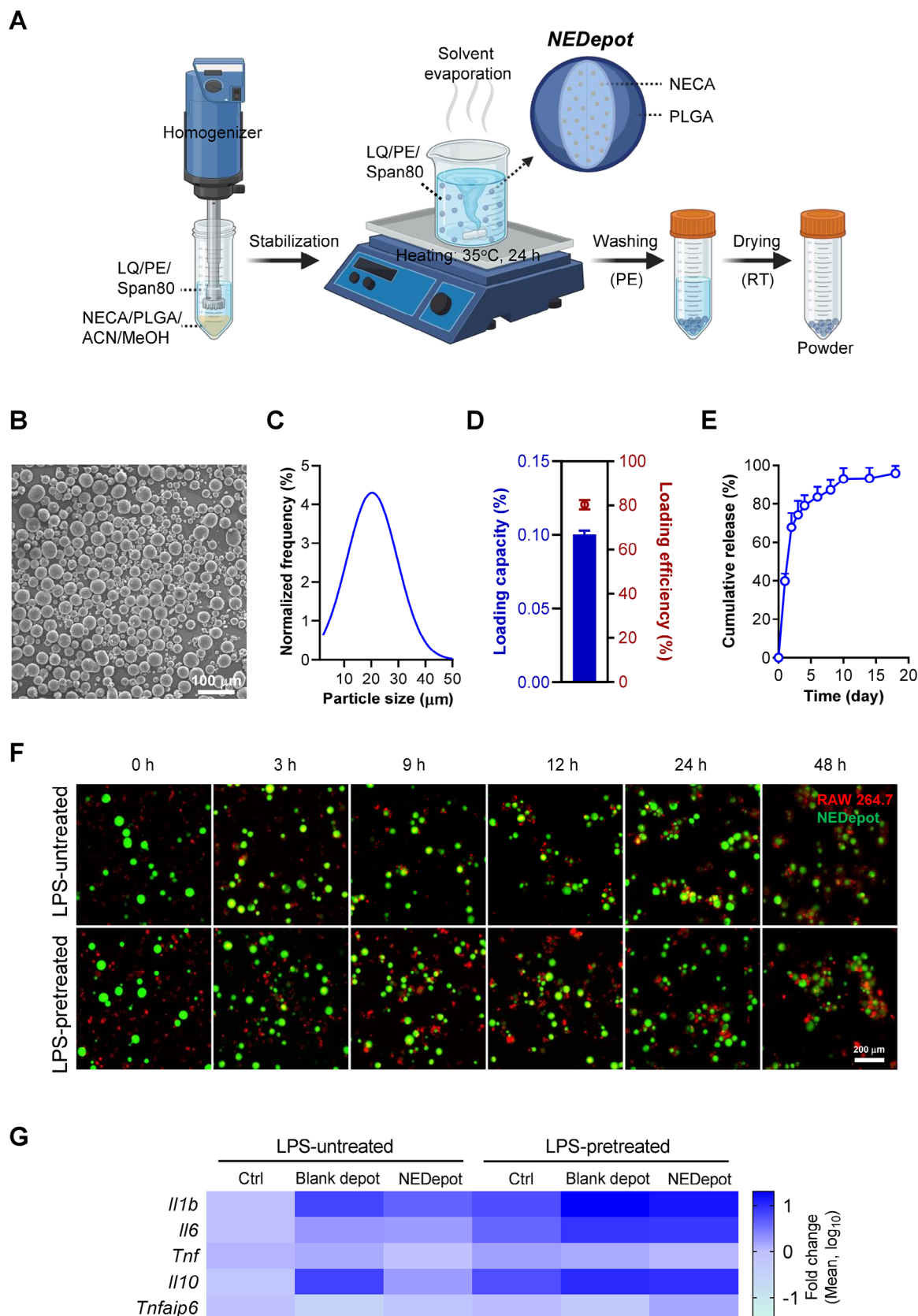
FIGURE 2 Development of 5′-(N-ethylcarboxamido) adenosine (NECA)-loaded poly(lactic-co-glycolic acid) micro-depots (NEDepot) for single localized NECA delivery. (A) The scheme illustrating NEDepot fabrication. ACN, acetonitrile; MeOH, methanol; PLGA, poly(lactic-co-glycolic acid). (B and C) Scanning electron microscopy image of NEDepot (B) and quantified particle size (C). Scale bar: 30 µm. (D) Physical characteristic analysis of NEDepot. (E) Sustained release pattern of NECA from NEDepot in vitro. (F) Representative images

correlation between the representative genes in the gene set is significantly more robust in the MI situation, and the correlation is weakened when treated with NEDepot. This suggests that the genes may be representative of the MI condition, and their expression returns to normal when the MI condition improves (Figure 4C). In summary, the GSEA results showed that NEDepot had a therapeutic effect by restoring normal cardiac function and homeostasis, reducing inflammatory response and oxidative stress, and enhancing mitochondrial function.

3.5 | NEDepot mitigated myocardial damage via multiple cardiac benefits post-MI

To further validate the therapeutic effects of NEDepot, heart samples were subjected to the histological and immunohistochemistry staining. MI hearts exhibited markedly necrosis and fibrosis, accompanied by cardiomyocyte hypotrophy (Figures 5A,B and S5A,B), while hearts under NEDepot treatment exhibited ameliorated response. Such findings were consistently observed in the apoptosis and oxidation analysis (Figures 5C and S5C). To confirm the angiogenic characteristic of NEDepot in vivo, CD31-positive ECs were evaluated in the LV (infarcted zone) of hearts (Figure 5D). Both MI hearts exhibited evidently reduced CD31-positive EC density in the infarcted zone, but hearts in MI + NEDepot group showed enhancement in the CD31 positivity (Figure 5F). Consistent with CD31, we assessed vascular endothelial growth factor (VEGF)-A expression in the border region between normal and infarcted LV myocardium (Figure 5E). MI + NEDepot mice displayed significantly elevated VEGF expression, compared to Sham and MI mice (Figure 5F), highlighting promoted revascularization. Meanwhile, vascular smooth muscle cells, marked by alpha-Smooth Muscle Actin (α-SMA), in MI + NEDepot hearts also displayed diminished damage, indicating the reservation of vascular integration and function, supporting the amelioration of NEDepot on MI-induced cardiac injury. For further verification, cardiac lysates were subjected to immunoblot analysis (Figure 5G). NEDepot-treated MI hearts exhibited decreased α-SMA supporting the reduction in fibrosis. In consist, cardiac damage marker (cTnI) and apoptotic markers (p53 and c-cas 3) were also downregulated in NEDepot-treated MI hearts.

NEDepot promoted VEGF-A expression at the protein levels further verified its angiogenic property (Figures 5H and S5D). The gap junction organization was perturbed in both MI hearts but was evidently attenuated under NEDepot treatment (Figure 5I). Notably, we assessed key circulatory factors indicating the degree of injury in multiorgans, including heart, liver, and kidney, that are highly sensitive to MI-induced hemodynamics decline and systemic inflammatory mediator release (Figure 5J). Their reduced expression under NEDepot treatment validated the systemic benefits of NEDepot during MI progression, both in heart damage and in multi-organ complications. This finding also emphasized that NEDepot administration did not exert adverse effects on hepatic function while being metabolized by liver, highlighting its biosafety and viability.

To evaluate the long-term therapeutic effects of NEDepot, we conducted an independent experiment assessing myocardial indices at 4-week post-MI. Electrocardiography analysis revealed profound alterations in HR and rhythm in vehicle-treated MI mice, which were reversed by NEDepot injection (Figure S6A). Similarly, NEDepot-treated MI mice exhibited substantial improvements in LV systolic function (Figure S6B), preventing further myocardial injury as MI progressed and mitigating cardiac remodeling (Figure S6C,D). These findings emphasize the systemic benefits of NEDepot in infarcted myocardium, demonstrating its comprehensive roles in ameliorating early myocardial damage and attenuating disease progression throughout MI.

3.6 | NECA attenuated cardiac injury by enhancing mitostasis

Considering that NEDepot modulated gene expression related to mitochondrial metabolism and demonstrated multifaceted benefits in mitigating MI progression, we further evaluated the interplay between NECA and AMPK, a master regulator of multiple critical processes including mitochondrial dynamics,[22] inflammation,[23] and angiogenesis.[24] Protein docking modeling was employed to evaluate the potential interaction between NECA and AMPKγ binding subunit (Figure 6A). The three possible binding modes indicated the affinity and strength of the interaction between AMPK and NECA, implying the potential of NECA on the binding with AMPK (Figure S7).

---

illustrating the interaction between NEDepot (marked with Coumarin-6, green) and macrophages (RAW 264.7, Dil-1,1′-dioctadecyl-3,3,3′,3′-tetramethyl-indocarbocyanine perchlorate [Dil], red) with or without lipopolysaccharide (LPS) pre-treatment. Scale bar: 200 μm. (G) NEDepot-induced inflammatory gene expressions declined in macrophages with or without LPS pre-treatment. *Il10*: interleukin 10, *Tnfaip6*: TNF alpha-induced protein 6. Data (D and E) represent the mean ± SEM ($n = 3$).
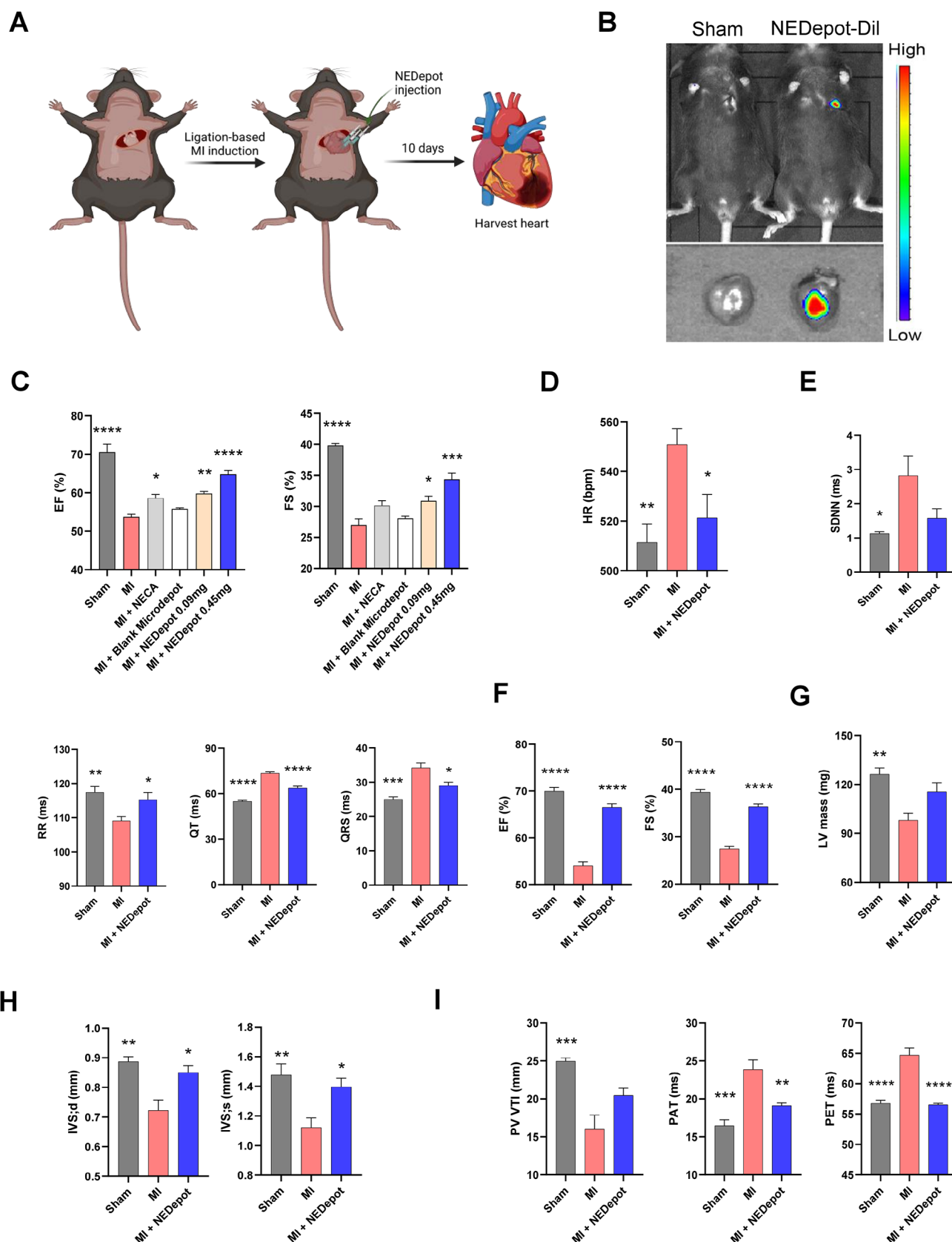
FIGURE 3 Local administration of 5′-(N-ethylcarboxamido) adenosine (NECA)-loaded poly(lactic-co-glycolic acid) micro-depots (NEDepot) within infarcted myocardium prevented cardiac dysfunction post-myocardial infarction (MI). (A) Schematics of MI modeling and NEDepot localized injection. (B) In Vivo Imaging Spectrum (IVIS) imaging of local NEDepot (marked with Cy5.5) injection. (C) Echocardiogram of mice at 10 days post-MI. EF, ejection fraction; FS, fraction shortening. (D and E) Electrocardiography analysis. HR, heart

To verify this, we examined the effects of NECA on cardiomyocytes, in both normoxic (Figures 6B and S8A) and hypoxic (Figures 6C and S8B) conditions. NECA induced a remarkable elevation of p-AMPKα expression in dose- and time-dependent manners. Additionally, NECA-treated cardiomyocytes exhibited elevated expression of *Ppargc1a* and *Tfam* genes, highlighting its advance in mitochondrial function (Figure 6D). This observation aligned with the enhanced oxygen consumption rate induced by NECA (Figure 6E), with both basal and maximal respiration, along with ATP production, in comparison to hypoxic cardiomyocytes (Figure 6F).

For further validation, we generated the AMPKγ2-KO H9c2 cardiomyocytes (#1–3) via CRISPR/Cas9 gene editing. Immunoblot analysis confirmed partial KO of AMPKγ2 in #3 H9c2 cells, and almost complete KO in #1 H9c2 cells (Figure 6G), substantiated by sequencing analysis (Figures 6H,I and S9). AMPKγ2-ablated H9c2 cells exhibited normal viability in normoxic condition, however, the cardioprotective effects of NECA against hypoxia declined in #3 cells, with a further reduction observed in #1 cells, compared to normal hypoxic H9c2 cells under NECA treatment (Figure 6J,K). This was further evidenced by immunoblot analysis, where NECA-treated hypoxic #3 H9c2 cells displayed increased expression of cell damage markers, with a further elevation in NECA-treated #1 cells (Figure 6L). Notably, corresponding to the AMPKγ2 expression, p-AMPKα expression levels in #3 H9c2 cells treated with $CoCl_2$ and NECA was partially declined when compared to those in normal cells, while #1 cells demonstrated a more pronounced reduction. Given the pivotal role of p65 phosphorylation in the inflammatory response,[25] we assessed the expression levels of p-p65 in these two AMPKγ2-KO cells, with the results revealing a distinct enhancement under hypoxic conditions, particularly in #1 H9c2 cells, regardless of NECA treatment. Consistently, AMPKγ2 deletion attenuated NECA-induced elevation of PGC-1α-targeted genes (*Esrra* and *Ppara*) in H9c2 cells, implying the lack of mitochondrial modulation by NECA in the absence of AMPK (Figure 6M). These findings were corroborated by complementary in vivo investigations. NEDepot promoted AMPK phosphorylation while suppressing p-p65 expression in infarcted myocardium (Figure S10A–C). Likewise, NEDepot upregulated the expression of mitostasis-related transcription factors (Figure S10D,E). Taken together, our investigations substantiate that NECA attenuates cardiac injury by enhancing mitostasis via AMPKα phosphorylation and PGC-1α activation.

4 | DISCUSSION AND CONCLUSION

Precision medicine has revolutionized therapeutic paradigms by emphasizing tailored treatments to address challenges such as off-target effects, limited efficacy, and suboptimal drug delivery systems. To overcome these limitations, advanced delivery platforms, including self-assembled nanoparticles, polymeric nanostructures, microspheres, and hydrogels, have emerged as promising tools for achieving localized, sustained, and targeted therapeutic outcomes. These cutting-edge materials are widely employed in the treatment of diverse pathologies, such as cancer,[26] osteoarticular diseases,[27] and ischemic cardiovascular disease,[28] due to their ability to enhance drug stability, bioavailability, and specificity. Building on these advancements, novel strategies for MI therapies have been actively developed. Supramolecular self-assembled nanoparticles have been applied to protect myocardium from injury and fibrosis.[29] Intravenous administration of ion cocktail with multifaceted benefits has shown promise in reducing infarction, promoting ischemic angiogenesis, and alleviating cardiac remodeling post-MI.[30] Cardiac patches composed of scaffolds or therapeutic agent-loaded systems offer mechanical reinforcement, synchronized electrical conduction, and localized delivery to facilitate myocardial repair.[31] These approaches address the challenges posed by the acute and complex pathophysiology of MI, where rapid intervention and sustained therapeutic efficacy are critical for improving clinical outcomes. Nonetheless, the multifaceted nature of MI demands continued innovation to achieve comprehensive systemic therapeutic benefits and localized precision.

In previous studies, the adenosine agonist NECA displayed significant promotion in tissue restitution and revascularization, indicating its promising potential in MI treatment.[14,32] Considering the urgency of MI treatment and the potential side effects of adenosine, herein we employed biodegradable PLGA microspheres to locally deliver NECA, so called NEDepot, within the infarcted myocardium via IMI. Though several nano/micro-formulations have been studied for the delivery of adenosine and its derivatives, they exhibited of very

---

rate; SDNN, standard deviation of normal-to-normal. (F–I) Echocardiogram of mice indicating cardiac systolic function (F), left ventricular (LV) mass (G), structural alteration (H), and hemodynamics parameters of right ventricle (I). d, diastole; IVS, interventricular septum; PAT, pulmonary artery acceleration time; PET, pulmonary artery ejection time; PV VTI, pulmonary valve velocity time integral; s, systole. *$p < .05$, **$p < .01$, ***$p < .001$, ****$p < .0001$ versus MI group. Data represent the mean ± SEM ($n = 5$), by one-way analysis of variance (ANOVA).
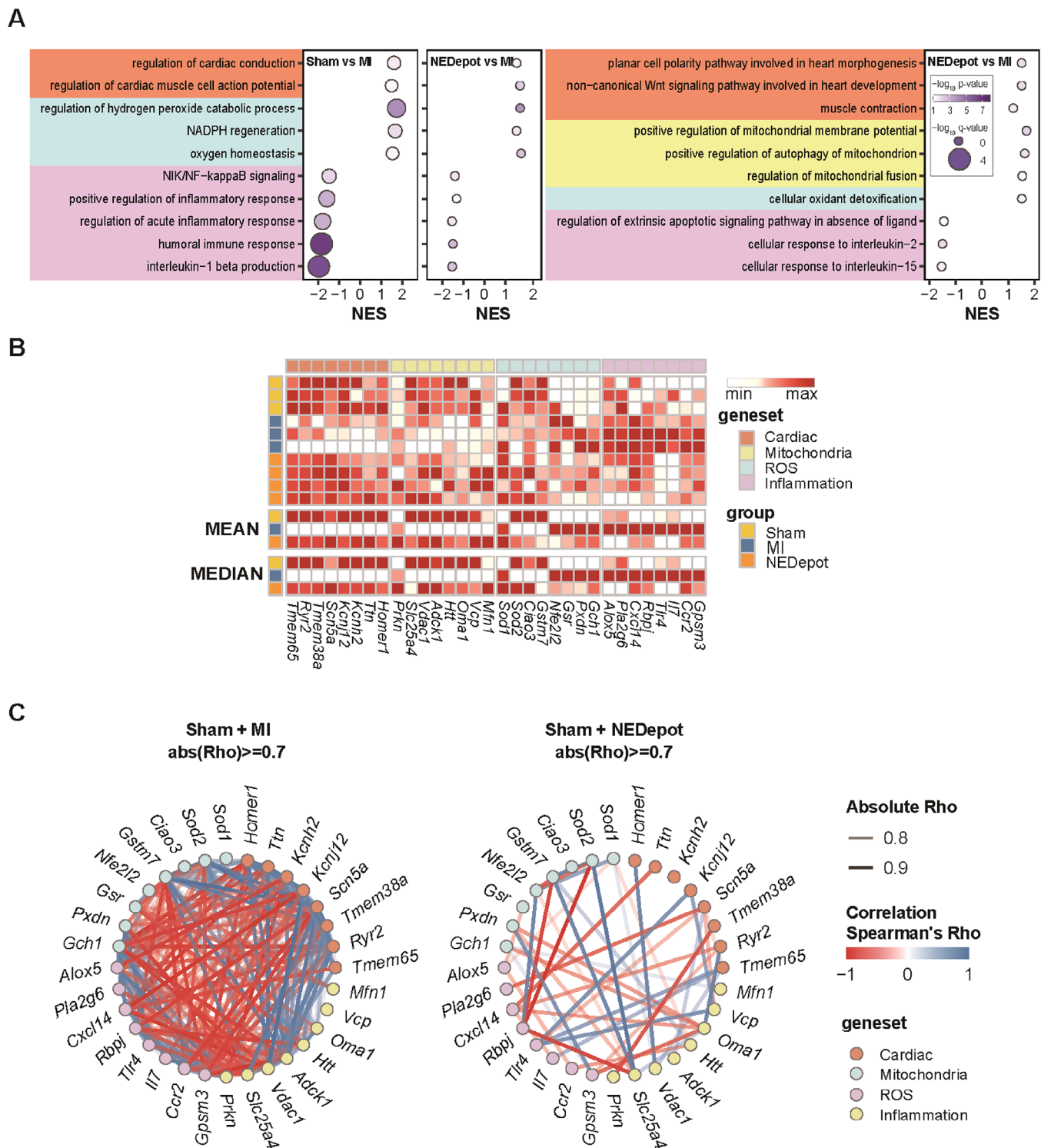
FIGURE 4 Ameliorated cardiac injury by 5′-(N-ethylcarboxamido) adenosine (NECA)-loaded poly(lactic-co-glycolic acid) micro-depots (NEDepot) administration is attributable to regulation of gene sets of cardiac homeostasis, mitochondria, oxidative stress, and inflammation. (A) Bubble plots summarizing the significantly altered gene sets as results of gene set enrichment analysis (GSEA). (B) A heatmap showing differential gene expression among different groups, which correlates with cardiac function and homeostasis, mitochondria, reactive oxygen species (ROS), and inflammation. (C) Gene network summarizing the correlations among representative genes of gene sets related to cardiac function and homeostasis, mitochondria, ROS, and inflammation.
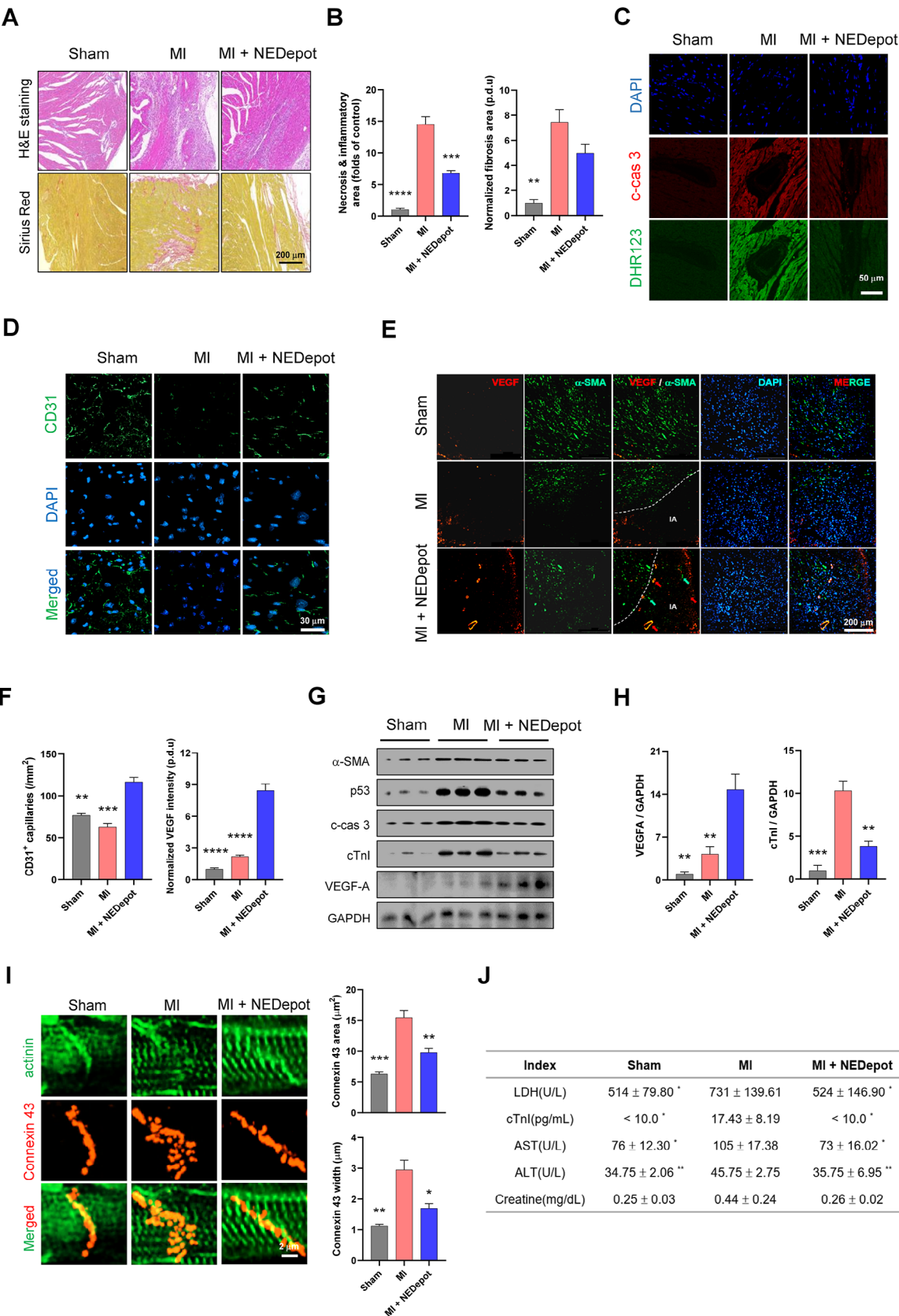
Index	Sham	MI	MI + NEDepot
LDH(U/L)	514 ± 79.80 *	731 ± 139.61	524 ± 146.90 *
cTnI(pg/mL)	< 10.0 *	17.43 ± 8.19	< 10.0 *
AST(U/L)	76 + 12.30 *	105 ± 17.38	73 + 16.02 *
ALT(U/L)	34.75 ± 2.06 **	45.75 ± 2.75	35.75 ± 6.95 **
Creatine(mg/dL)	0.25 ± 0.03	0.44 ± 0.24	0.26 ± 0.02

FIGURE 5 5′-(N-ethylcarboxamido) adenosine (NECA)-loaded poly(lactic-co-glycolic acid) micro-depots (NEDepot) mitigated myocardial infarction (MI)-induced myocardial damage through the reduction of apoptosis, fibrosis, inflammation, and oxidation, as well as the promotion of angiogenesis. (A and B) Representative images of hematoxylin and eosin (H&E) and Sirius Red staining of cardiac sections ($n = 3$). Scale bar: 100 μm. (C) Representative images for apoptotic (c-cas, red) and oxidative marker (DHR123, green) staining in cardiac

low drug loading efficiency and short drug release time due to high or partial water-soluble properties of these compounds.[33] The presence of water in the aqueous emulsion fabrication would lead to high leak of drugs to the external phase. To overcome this limitation, we developed a novel approach to control high loading efficacy of NECA using the oil-in-oil emulsion method. This method can be utilized to fabricate micro-depots of drugs belonging to water-soluble group.[34] In addition, NEDepot with the size of 10–40 μm showed good injectability and escaping from phagocytosis of macrophages, thereby maintaining their localization in the injured sites to allow complete drug release and enhancing its specificity and effectiveness. Notably, employing PLGA as NECA delivery vehicle manifests multifaced benefits such as tunable release rates, biocompatibility, and stability, with an emphasizing of its biodegradable nature avoiding additional damage of local administration, providing promising availability in further clinical therapeutic applications.

In this study, we characterized the phenotypes of NEDepot-treated MI mice, substantiated that NEDepot evidently improved myocardial function within the early phase of MI, with a pronounced elevation in comparison to free NECA injection, representing the advantages of controlled release. Consistently, IMI of NEDepot facilitated the restoration of cardiac rhythm and the modulation of intrinsic automaticity in the compromised heart, contributing to enhanced cardiac stability. Notably, in the clinical setting, the majority of severe patients with MI generally characterized by multi-vessel involvement and segmental stenosis, with vary infarcted locations among different patients. Traditional drug therapies, in this context, have limited efficacy and lack specificity to address the focal myocardial ischemia. Paradoxically, the utilization of high-dose positive inotropic agents, such as dopamine and epinephrine, to maintain cardiac output and pulsation, may precipitate complications including arrhythmias and peripheral circulation disturbances, which, in turn, adversely impact patient prognosis.[35] Therefore, this study not only introduces the effects of adenosine agonist on significantly improving cardiac function and mitigating injury, but also underscores the paramount significance of locally delivered NEDepot into specific infarcted sections in the context of future clinical treatments, which holds great promise for facilitating personalized patient therapy.

Coronary artery occlusion-induced cellular coagulative necrosis triggers inflammatory response and oxidative stress.[36] The release of inflammatory factors and the excessive accumulation of free radicals are mutually causal, initiating lipid peroxidation, triggering DNA strand breaks and cardiomyocyte apoptosis, culminating in cardiac remodeling and heart failure.[37] Considering the intricate interplay within this cascade, our inclination leans toward the utilization of multi-target drug with comprehensive therapeutic potential in MI therapy. We believe that this strategy allows for a holistic intervention, effectively reducing the potential for drug interactions and the burden on the organism associated with the concurrent use of multiple medications, so as to synergistically regulate the complex biological processes following MI. Herein, NEDepot administration evidently reduced the expression of inflammatory and oxidative factors, while augmenting VEGF expression within the infarcted area, expediting microcirculation restoration and ameliorating progressive damage. The synergistic interactions effectively forestalled cardiomyocyte apoptosis and subsequent myocardial fibrosis, thus allowing the prominent cardioprotective effects of NEDepot in the early phase of MI. Together, local administration of NEDepot improves MI-induced cardiac injury and promotes myocardial recovery via multi-curative benefits, demonstrating promising prospects in further clinical therapy.

Mitostasis, the equilibrium of mitochondrial dynamics encompassing processes, has emerged as a critical determinant of cellular health and resilience in stress-induced pathologies such as MI. Recent studies have highlighted the central role of mitostasis in coordinating mitochondrial biogenesis, dynamics, and mitophagy to preserve energy homeostasis and reduce oxidative stress in ischemic tissues.[38] In this context, therapeutic strategies restoring mitostasis have exhibited promise in alleviating MI-induced damage and facilitating recovery. AMPK, a central regulator of energy metabolism, is known to be activated under conditions such as metabolic disorders and high energy demand,[39] functioning pivotal roles in mitostasis .[40] Given that the altered gene sets and observed phenotypes in response to NEDepot are closely associated with mitostasis, we mechanistically investigated NECA's mode of action by focusing on its interaction with AMPK. Notably, AMPK activation could trigger

---

sections from infarcted region. Scale bar: 50 μm. DHR, dihydrorhodamine. (D) Representative images for CD31 (green) and DAPI (blue) in cardiac sections from infarcted region. Scale bar: 30 μm. (E) Representative images for VEGF (red) and α-SMA (green) in cardiac sections from border region between infarcted and normal myocardium. Scale bar: 200 μm. (F) Quantifications of CD31$^+$ capillaries and VEGF intensity ($n = 3$). (G and H) Immunoblotting of cardiac lysates ($n = 3$). (I) Representative images for α-Actinin (green) and Connexin 43 (red) in cardiac sections from infarcted region. Scale bar: 2 μm. (J) Biochemistry analysis of serum ($n = 5$). $*p < .05$, $**p < .01$, $***p < .001$, $****p < .0001$ versus vehicle-treated (B and I) or NEDepot-treated (F and H) MI group. Data represent the mean ± SEM, by one-way analysis of variance (ANOVA).
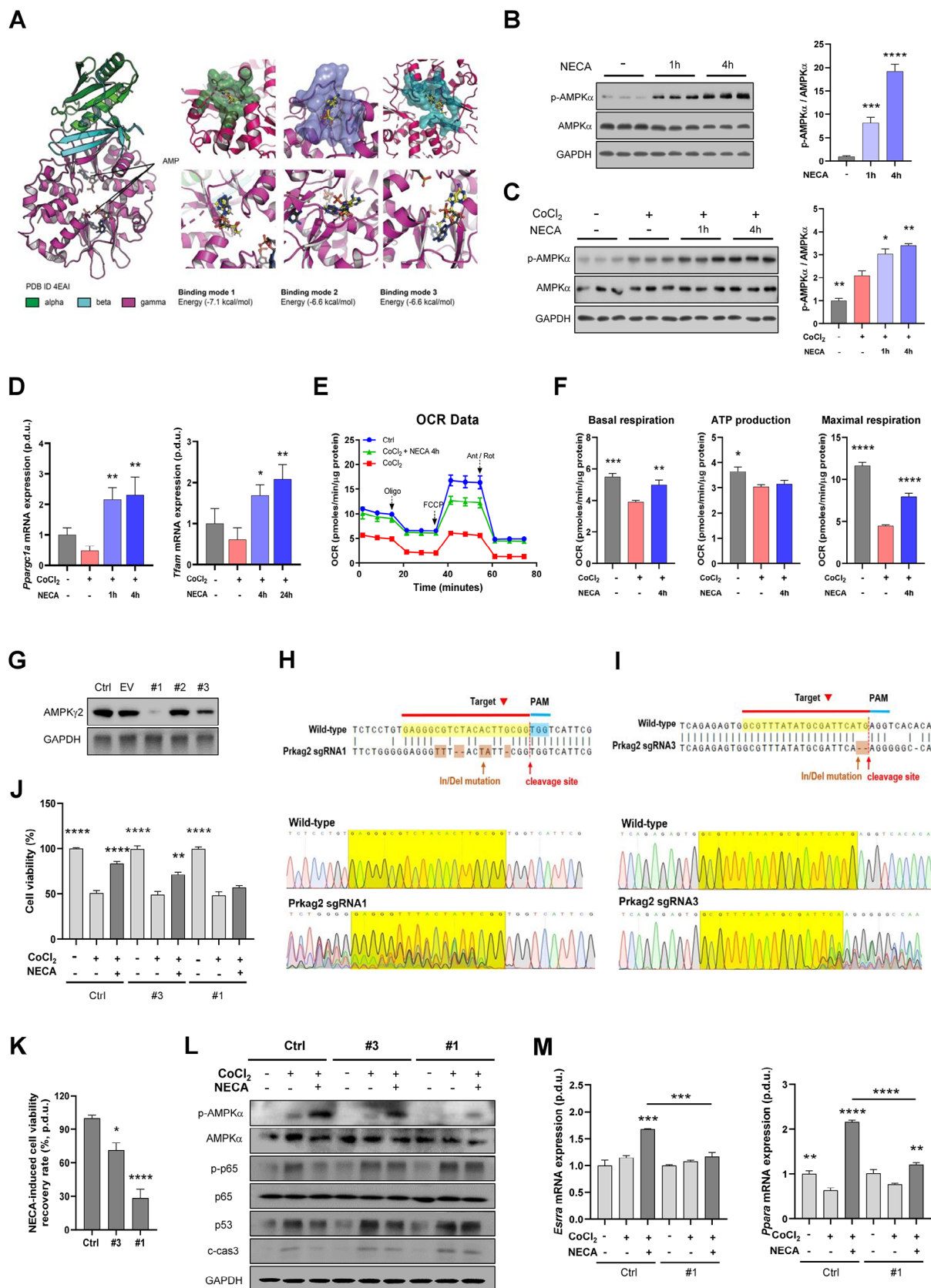
FIGURE 6 5′-(N-ethylcarboxamido) adenosine (NECA) attenuated cardiac injury by triggering mitostasis. (A) Docking simulation of NECA into AMP-activated protein kinase γ (AMPKγ) subunit. The alpha, beta, and gamma subunit of AMPK were colored green, cyan, and magenta, respectively. The three AMP molecules were represented by ball and stick model and label. The NECA molecules painted by yellow color. The nitrogen, oxygen, and phosphate molecules were colored blue, red, and orange, respectively. The binding pose of NECA were

PGC-1α signaling, a crucial inducible transcriptional coactivator essential for cardiac function. Specifically, PGC-1α contributes to mitostasis by enhancing mitochondrial biogenesis, regulating enzyme expression, and modulating Tfam, a critical factor for transcription and replication of mitochondrial genome.[41] In our study, NECA was corroborated to interconnect with AMPKγ binding region, leading to the phosphorylation of catalytic AMPKα subunit and subsequently activation of the AMPK–PGC-1α–Tfam cascade. These findings highlight the significance of NECA in ameliorating mitostasis and propose its therapeutic implications in MI therapy. Significantly, PGC-1α has been identified as a coactivator for ERR and PPAR, the pivotal regulators of myocardial FA utilization.[42] This orchestrated cascade, in conjunction with the relief of CPT1 inhibition facilitated by AMPK activation,[43] serves to enhance the FAO process and coupled respiration. This mechanism contributes to the amelioration of energy metabolism and reduction in lactate production, consequently mitigating cardiomyocyte death. Our study substantiated that NECA upregulated the transcriptional levels of PPARα and ERRα under hypoxia, which was reversed in the context of AMPKγ ablation, underscoring the cardioprotective and mitochondria regulatory effects of NECA are performed via AMPK activation. In addition, AMPK is well documented to exert anti-inflammatory effects[44] and promote angiogenesis,[45] both of which are consistent with the NEDepot-induced phenotypes observed in vivo. This alignment further supports the rationale for selecting AMPK as a potential target of NECA. Mechanistically, NECA modulates inflammatory responses by activating AMPK, which subsequently suppresses nuclear factor-kappa B (NF-κB) signaling, leading to a reduction in inflammatory cytokine expression. This inhibition was abolished in the absence of AMPKγ, highlighting the AMPK–NF-κB cascade as a critical pathway underlying NECA's anti-inflammatory properties. Likewise, p65 activation has been shown to

increase interaction with PGC-1α, resulting in the reduction of PGC-1α expression.[46] This provides supportive evidence for NECA-induced elevation of PGC-1α, revealing the intricate and interactive nature of intracellular signaling pathways. Nevertheless, the specific molecular mechanisms underlying the pro-angiogenic impacts of NECA in different cell types remain to be further explored in subsequent studies. In addition to its intracellular activities, NECA, functioning as a non-specific adenosine agonist, could also directly bind to adenosine receptors, initiating diverse downstream signaling pathways, typified by the PKA–CREB–PGC-1α cascade, which has been well elucidated previously.[41,47] Activated adenosine receptors stimulate adenylyl cyclase, resulting in cAMP production and PKA activation. This cascade culminates in the phosphorylation of CREB, facilitating its translocation to the nucleus, and subsequently upregulating PGC-1α gene transcription. These findings align with our results, supporting the enhancement of mitostasis by NECA.

Considering the translation of experimental results into further clinical applications, we believe that intramyocardial delivery of NEDepot addresses several limitations of current therapeutic strategies. IMI of NEDepot offers a localized and sustained delivery system that circumvents the challenges of systemic drug administration, such as off-target effects and rapid clearance. By focusing treatment directly within the infarcted myocardium, this approach enhances drug bioavailability at the site of injury, facilitating optimal therapeutic outcomes. The distinct pharmacological profile of NEDepot underscores its potential to ameliorate MI-triggered cardiac damage, enhance myocardial resilience, as well as providing sufficient cardiac support within the early phase of MI to reduce the risk of perioperative MI recurrence and other related cardiac events. Notably, NEDepot injection therapy may be especially beneficial for patients contraindicated for traditional interventions such as percutaneous

---

compared with the binding mode of AMP by superposing two molecules. The green, purple, and cyan surfaces were represented for the residues involved in NECA interaction of binding modes 1–3. (B and C) Immunoblotting of cardiomyocytes in normoxic (B) and hypoxic condition (C) treated with NECA at 100 μM. (D) The mRNA expression level in cardiomyocytes under hypoxic condition in response to NECA treatment. *Ppargc1*: peroxisome proliferator-activated receptor-γ coactivator 1-α, *Tfam*: transcription factor A, mitochondrial. (E) Oxygen consumption rate (OCR) analysis. Ant, antimycin; FCCP, carbonyl cyanide-4 (trifluoromethoxy) phenylhydrazone; Oligo, oligomycin; Rot, rotenone. (F) Basal and maximal respiration-related and ATP production-related oxygen consumption. (G) Immunoblot assay validating AMPKγ2 deletion in H9c2 cells. (H and I) Sanger sequencing validating the indels in #1 (H) and #3 (I) AMPKγ2-KO H9c2 cells. Each indel that was identified by fragment analysis was sequenced using the Sanger method to establish the correlation between fragment analysis and Sanger sequencing data. (J) Cell viability assay of AMPKγ2-KO H9c2 cells. (K) NECA-induced cell viability recovery rate, assessed by the normalized viability proportion of the difference between cells co-treated with NECA and CoCl$_2$ versus cells treated with CoCl$_2$. (L) Immunoblot analysis of normal and AMPKγ2-KO H9c2 cells. (M) The mRNA expression of mitostasis-related genes (*Esrra* and *Ppara*) in response to NECA treatment. *Esrra*: estrogen-related receptor alpha, *Ppara*: peroxisome proliferator activated receptor alpha. $*p < .05$, $**p < .01$, $***p < .001$, $****p < .0001$ versus untreated (B and K) or CoCl$_2$-treated (C–F and J–M) group. Data (B–F and J–M) represent the mean $\pm$ SEM ($n = 3$), by one-way analysis of variance (ANOVA).

coronary intervention or coronary artery bypass grafting. In scenarios where surgical approaches are unfeasible due to comorbidities, severe bleeding tendencies, or advanced multi-organ dysfunction,[48] NEDepot provides a minimally invasive alternative with a high therapeutic index. Furthermore, its compatibility with personalized medicine is noteworthy, as the localized delivery system can be tailored to target specific infarcted regions, thereby minimizing systemic toxicity and enhancing patient-specific outcomes. These potential applications emphasize the significance and perspectives of NEDepot, providing novel avenues in advanced clinical treatment for patients with MI. Future works should be optimizing the method to fabricate NEDepot with high uniformity in size, which allows to control the drug dose and release pattern. Microfluidic fabrication or membrane emulsification could be good options in this aspect.[49] In addition, NEDepot can be incorporated into heart-adhesive patches to prevent injection-associated side effects.

AUTHOR CONTRIBUTIONS

Dongryeol Ryu and Jee-Heon Jeong conceived and designed the project. Shibo Wei, Tiep Tien Nguyen, Yan Zhang, Wonyoung Park, and Nhu-Nam Nguyen performed the experiments. Yunju Jo carried out bioinformatics analysis. Chang-Myung Oh, Jin Han, Doyoun Kim, and Ki-Tae Ha provided valuable comments and supervision. Shibo Wei, Tiep Tien Nguyen, and Yan Zhang analyzed data and wrote the manuscript. Dongryeol Ryu and Jee-Heon Jeong managed the experiment progression and revised the manuscript.

CONFLICT OF INTEREST STATEMENT

The authors declare no conflict of interest.

DATA AVAILABILITY STATEMENT

RNA sequencing data are available at the United States National Center for Biotechnology Information Gene Expression Omnibus repository under accession number GSE270433. The datasets used and/or analyzed during the current study are available from the corresponding author on reasonable request.

ORCID

Dongryeol Ryu https://orcid.org/0000-0001-5905-6760

REFERENCES

1. G. W. Reed, J. E. Rossi, C. P. Cannon, *Lancet* **2017**, *389*, 197.
2. S. Frantz, M. J. Hundertmark, J. Schulz-Menger, F. M. Bengel, J. Bauersachs, *Eur. Heart J.* **2022**, *43*, 2549.
3. a) Q. Sun, H. Ma, J. Zhang, B. You, X. Gong, X. Zhou, J. Chen, G. Zhang, J. Huang, Q. Huang, Y. Yang, K. Ai, Y. Bai, *Adv. Sci.* **2023**, *10*, e2204999; b) K. Wang, L. Y. Zhou, F. Liu, L. Lin, J. Ju, P. C. Tian, C. Y. Liu, X. M. Li, X. Z. Chen, T. Wang, F. Wang, S. C. Wang, J. Zhang, Y. H. Zhang, J. W. Tian, K. Wang, *Adv. Sci.* **2022**, *9*, e2106058.
4. a) T. J. Cahill, R. P. Choudhury, P. R. Riley, *Nat. Rev. Drug Discov.* **2017**, *16*, 699; b) M. Writing Committee, G. J. Dehmer, C. L. Grines, F. G. Bakaeen, D. L. Beasley, T. M. Beckie, J. Boyd, J. E. Cigarroa, S. R. Das, R. L. Diekemper, J. Frampton, C. N. Hess, N. Ijioma, J. S. Lawton, B. Shah, N. R. Sutton, *J. Am. Coll. Cardiol.* **2023**, *82*, 1131.
5. L. C. Liew, B. X. Ho, B. S. Soh, *Stem Cell Res. Ther.* **2020**, *11*, 138.
6. C. Puelacher, D. M. Gualandro, N. Glarner, G. Lurati Buse, A. Lampart, D. Bolliger, L. A. Steiner, M. Grossenbacher, K. Burri-Winkler, H. Gerhard, E. A. Kappos, O. Clerc, L. Biner, Z. Zivzivadze, C. Kindler, A. Hammerer-Lercher, M. Filipovic, M. Clauss, L. Gurke, T. Wolff, E. Mujagic, M. Bilici, F. A. Cardozo, S. Osswald, B. Caramelli, C. Mueller, B.-P. Investigators, *Eur. Heart J.* **2023**, *44*, 1690.
7. P. A. Borea, S. Gessi, S. Merighi, F. Vincenzi, K. Varani, *Physiol. Rev.* **2018**, *98*, 1591.
8. a) G. G. Yegutkin, D. Boison, *Pharmacol. Rev.* **2022**, *74*, 797; b) P. Kofuji, A. Araque, *Neuroscience* **2021**, *456*, 71; c) R. D. Leone, L. A. Emens, *J. Immunother. Cancer* **2018**, *6*, 57.
9. a) A. Davila, Y. Tian, I. Czikora, S. W. A, N. Weinand, G. Dong, J. Xu, J. Li, H. Su, G. Kapuku, Y. Huo, Z. Bagi, *Microcirculation* **2020**, *27*, e12624; b) M. C. Procopio, R. Lauro, C. Nasso, S. Carerj, F. Squadrito, A. Bitto, G. Di Bella, A. Micari, N. Irrera, F. Costa, *Biomedicines* **2021**, *9*, 204.
10. R. Guieu, J. C. Deharo, B. Maille, L. Crotti, E. Torresani, M. Brignole, G. Parati, *J. Clin. Med.* **2020**, *9*, 1366.
11. J. F. Chen, H. K. Eltzschig, B. B. Fredholm, *Nat. Rev. Drug Discov.* **2013**, *12*, 265.
12. a) A. Bahreyni, M. Khazaei, M. Rajabian, M. Ryzhikov, A. Avan, S. M. Hassanian, *J. Pharm. Pharmacol.* **2018**, *70*, 191; b) A. Z. El-Hashim, H. T. Abduo, O. M. Rachid, Y. A. Luqmani, B. Y. Al Ayadhy, G. M. Alkhaledi, *Pulm. Pharmacol. Ther.* **2009**, *22*, 243.
13. a) M. Hormozi, S. Talebi, A. H. Zarnani, M. Jeddi-Tehrani, L. H. Gohari, H. Soltanghoraei, M. Jafarabadi, M. M. Akhondi, *Fertil. Steril.* **2011**, *95*, 2560; b) X. Du, X. Ou, T. Song, W. Zhang, F. Cong, S. Zhang, Y. Xiong, *Exp. Biol. Med.* **2015**, *240*, 1472.
14. T. T. Nguyen, F. Emami, S. Yook, H. T. Nguyen, T. T. Pham, S. Pathak, S. Regmi, J. O. Kim, C. S. Yong, J. R. Kim, J. H. Jeong, *J. Control Release* **2020**, *321*, 509.

15. F. van den Akker, D. A. Feyen, P. van den Hoogen, L. W. van Laake, E. C. van Eeuwijk, I. Hoefer, G. Pasterkamp, S. A. Chamuleau, P. F. Grundeman, P. A. Doevendans, J. P. Sluijter, *Eur. Heart. J.* **2017**, *38*, 184.

16. a) A. C. Gaffey, M. H. Chen, C. M. Venkataraman, A. Trubelja, C. B. Rodell, P. V. Dinh, G. Hung, J. W. MacArthur, R. V. Soopan, J. A. Burdick, P. Atluri, *J. Thorac. Cardiovasc. Surg.* **2015**, *150*, 1268; b) S. Hu, D. Zhu, Z. Li, K. Cheng, *ACS Nano* **2022**, *16*, 15935; c) T. Hao, M. Qian, Y. Zhang, Q. Liu, A. C. Midgley, Y. Liu, Y. Che, J. Hou, Q. Zhao, *Adv. Sci.* **2022**, *9*, e2105408; d) Y. Liu, D. Zhong, Y. He, J. Jiang, W. Xie, Z. Tang, J. Qiu, J. Luo, X. Wang, *Adv. Sci.* **2022**, *9*, e2202920.

17. T. M. Yau, F. D. Pagani, D. M. Mancini, H. L. Chang, A. Lala, Y. J. Woo, M. A. Acker, C. H. Selzman, E. G. Soltesz, J. A. Kern, S. Maltais, E. Charbonneau, S. Pan, M. E. Marks, E. G. Moquete, K. L. O'Sullivan, W. C. Taddei-Peters, L. K. McGowan, C. Green, E. A. Rose, N. Jeffries, M. K. Parides, R. D. Weisel, M. A. Miller, J. Hung, P. T. O'Gara, A. J. Moskowitz, A. C. Gelijns, E. Bagiella, C. A. Milano, Cardiothoracic Surgical Trials Network, *JAMA* **2019**, *321*, 1176.

18. E. Gao, Y. H. Lei, X. Shang, Z. M. Huang, L. Zuo, M. Boucher, Q. Fan, J. K. Chuprun, X. L. Ma, W. J. Koch, *Circ. Res.* **2010**, *107*, 1445.

19. L. Chen, J. Wang, Y. Y. Zhang, S. F. Yan, D. Neumann, U. Schlattner, Z. X. Wang, J. W. Wu, *Nat. Struct. Mol. Biol.* **2012**, *19*, 716.

20. G. M. Morris, R. Huey, W. Lindstrom, M. F. Sanner, R. K. Belew, D. S. Goodsell, A. J. Olson, *J. Comput. Chem.* **2009**, *30*, 2785.

21. L. Jin, M. Cho, B. S. Kim, J. H. Han, S. Park, I. K. Lee, D. Ryu, J. H. Kim, S. J. Bae, K. T. Ha, *BMB Rep.* **2021**, *54*, 563.

22. S. Herzig, R. J. Shaw, *Nat. Rev. Mol. Cell Biol.* **2018**, *19*, 121.

23. Y. Xu, L. Bai, X. Yang, J. Huang, J. Wang, X. Wu, J. Shi, *Heliyon* **2024**, *10*, e33670.

24. Y. Li, R. Sun, J. Zou, Y. Ying, Z. Luo, *Cells* **2019**, *8*, 752.

25. S. C. Sun, *Nat. Rev. Immunol.* **2017**, *17*, 545.

26. J. Yang, Y. He, M. Zhang, C. Liang, T. Li, T. Ji, M. Zu, X. Ma, Z. Zhang, C. Liang, Q. Zhang, Y. Chen, L. Hou, *Exploration* **2023**, *3*, 20230061.

27. J. Zhou, Z. Zhang, J. Joseph, X. Zhang, B. E. Ferdows, D. N. Patel, W. Chen, G. Banfi, R. Molinaro, D. Cosco, N. Kong, N. Joshi, O. C. Farokhzad, C. Corbo, W. Tao, *Exploration* **2021**, *1*, 20210011.

28. D. Zhu, Z. Li, K. Huang, T. G. Caranasos, J. S. Rossi, K. Cheng, *Nat. Commun.* **2021**, *12*, 1412.

29. W. Guo, W. Feng, J. Huang, J. Zhang, X. Fan, S. Ma, M. Li, J. Zhan, Y. Cai, M. Chen, *ACS Appl. Mater. Interfaces* **2021**, *13*, 22131.

30. Y. Que, J. Shi, Z. Zhang, L. Sun, H. Li, X. Qin, Z. Zeng, X. Yang, Y. Chen, C. Liu, C. Liu, S. Sun, Q. Jin, Y. Zhang, X. Li, M. Lei, C. Yang, H. Tian, J. Tian, J. Chang, *Exploration* **2024**, *4*, 20230067.

31. T. Liu, Y. Hao, Z. Zhang, H. Zhou, S. Peng, D. Zhang, K. Li, Y. Chen, M. Chen, *Circulation* **2024**, *149*, 2002.

32. B. Csoka, Z. Selmeczy, B. Koscso, Z. H. Nemeth, P. Pacher, P. J. Murray, D. Kepka-Lenhart, S. M. Morris Jr., W. C. Gause, S. J. Leibovich, G. Hasko, *FASEB J.* **2012**, *26*, 376.

33. M. Kazemzadeh-Narbat, N. Annabi, A. Tamayol, R. Oklu, A. Ghanem, A. Khademhosseini, *J. Drug Target.* **2015**, *23*, 580.

34. a) T. T. Nguyen, C. D. Phung, J. O. Kim, C. S. Yong, J. R. Kim, S. Yook, J. H. Jeong, *J. Control Release* **2021**, *336*, 274; b) J. A. Champion, S. Mitragotri, *Proc. Natl. Acad. Sci. U. S. A.* **2006**, *103*, 4930.

35. T. Ahmad, P. E. Miller, M. McCullough, N. R. Desai, R. Riello, M. Psotka, M. Bohm, L. A. Allen, J. R. Teerlink, G. M. C. Rosano, J. Lindenfeld, *Eur. J. Heart Fail.* **2019**, *21*, 1064.

36. a) H. Xu, W. Yu, S. Sun, C. Li, J. Ren, Y. Zhang, *Sci. Bull.* **2021**, *66*, 1669; b) Q. Zhang, L. Wang, S. Wang, H. Cheng, L. Xu, G. Pei, Y. Wang, C. Fu, Y. Jiang, C. He, Q. Wei, *Signal Transduct. Target Ther.* **2022**, *7*, 78.

37. S. Zhong, L. Li, X. Shen, Q. Li, W. Xu, X. Wang, Y. Tao, H. Yin, *Free Radic. Biol. Med.* **2019**, *144*, 266.

38. a) C. J. A. Ramachandra, S. Hernandez-Resendiz, G. E. Crespo-Avilan, Y. H. Lin, D. J. Hausenloy, *EBioMedicine* **2020**, *57*, 102884; b) M. Zhou, Y. Yu, X. Luo, J. Wang, X. Lan, P. Liu, Y. Feng, W. Jian, *Cardiology* **2021**, *146*, 781.

39. S. Fu, *Sci. Bull.* **2017**, *62*, 1233.

40. E. Trefts, R. J. Shaw, *Mol. Cell* **2021**, *81*, 3677.

41. L. Chen, Y. Qin, B. Liu, M. Gao, A. Li, X. Li, G. Gong, *Front. Cell Dev. Biol.* **2022**, *10*, 871357.

42. J. M. Huss, D. P. Kelly, *J. Clin. Invest.* **2005**, *115*, 547.

43. J. R. Ussher, G. D. Lopaschuk, *Cardiovasc. Res.* **2008**, *79*, 259.

44. A. Salminen, J. M. Hyttinen, K. Kaarniranta, *J. Mol. Med.* **2011**, *89*, 667.

45. J. A. Reihill, M. A. Ewart, I. P. Salt, *Vasc. Cell* **2011**, *3*, 9.

46. I. Rabinovich-Nikitin, A. Blant, R. Dhingra, L. A. Kirshenbaum, M. P. Czubryt, *Cells* **2022**, 11, 2193.

47. P. J. Fernandez-Marcos, J. Auwerx, *Am. J. Clin. Nutr.* **2011**, *93*, 884S.

48. R. A. Byrne, X. Rossello, J. J. Coughlan, E. Barbato, C. Berry, A. Chieffo, M. J. Claeys, G. A. Dan, M. R. Dweck, M. Galbraith, M. Gilard, L. Hinterbuchner, E. A. Jankowska, P. Juni, T. Kimura, V. Kunadian, M. Leosdottir, R. Lorusso, R. F. E. Pedretti, A. G. Rigopoulos, M. Rubini Gimenez, H. Thiele, P. Vranckx, S. Wassmann, N. K. Wenger, B. Ibanez, ESC Scientific Document Group, *Eur. Heart J.* **2023**, *44*, 3720.

49. a) S. Yadavali, H. H. Jeong, D. Lee, D. Issadore, *Nat. Commun.* **2018**, *9*, 1222; b) W. Li, L. Zhang, X. Ge, B. Xu, W. Zhang, L. Qu, C. H. Choi, J. Xu, A. Zhang, H. Lee, D. A. Weitz, *Chem. Soc. Rev.* **2018**, *47*, 5646.

SUPPORTING INFORMATION

Additional supporting information can be found online in the Supporting Information section at the end of this article.